

1 **The role of biomass elemental composition and ion-exchange in metal sorption**
2 **by algae**

3 Ana R. F. Carreira,^a Telma Veloso,^{a,b} Inês P. E. Macário,^{a,b} Joana L. Pereira,^{a,b} Sónia P. M. Ventura,^a
4 Helena Passos,^{a*} João A. P. Coutinho^a

5 ^aCICECO - Aveiro Institute of Materials, Department of Chemistry, University of Aveiro, 3810-193
6 Aveiro, Portugal

7 ^bDepartment of Biology & CESAM, University of Aveiro, Aveiro, Portugal

8 *Corresponding author. Email: hpassos@ua.pt

9

10 **Abstract**

11 The use of macroalgae, microalgae and cyanobacteria for metal sorption has been widely
12 reported. Still, there are no studies allowing a direct comparison of the performance of these
13 biomasses, especially while evaluating metal competition. The simultaneous sorption of Co^{2+} ,
14 Cu^{2+} , Ni^{2+} and Zn^{2+} present in a multi-elemental solution by six macroalgae, two microalgae and
15 three cyanobacteria was evaluated. Brown macroalgae were shown to be the most promising
16 biosorbent, with *Undaria pinnatifida* having a total metal sorption capacity of $0.6 \text{ mmol}\cdot\text{g}^{-1}$.
17 Overall, macroalgae performed better than microalgae, followed by cyanobacteria. Carboxyl
18 groups were identified as being the main functional groups involved in metal sorption, and all
19 biomass samples were found to be selective to Cu^{2+} . This was linked not only to its higher
20 complexation constant value with relevant functional groups when compared to the remaining
21 metals, but also the Irving-Williams series. The release of K^{+} and Ca^{2+} to the aqueous solution
22 during the metal sorption was followed. The obtained results suggest they are readily exchanged
23 with metals in the solution, indicating the occurrence of an ion-exchange mechanism in metal
24 sorption by most biomass. Red macroalgae are an exception to the reported trends, suggesting
25 that their metal sorption mechanism may differ from the other biomass types.

26 **Keywords:** Macroalgae, microalgae, cyanobacteria, screening, sorption mechanism, metal
27 recovery.

28 **1. Introduction**

29 The strong dependence of modern societies on metal-rich commodities is putting pressure
30 on natural metal reserves.[1] To avoid short-term supply and demand constraints, the metal
31 industry must pursue a shift from a linear to a circular economy. Wastewaters such as industrial,
32 agricultural and municipal effluents are produced in large volumes and could be viable secondary
33 metal sources.[2–4] Wastewaters have an inherent organic and inorganic heterogeneity which
34 adds complexity to these matrices. Recovering metals from wastewater can be achieved using
35 processes such as hydrometallurgy, electrodeposition, membranes, bioleaching, chemical
36 precipitation and (bio)sorption.[4] Hybrid methodologies can also be developed by combining
37 different processes for better efficiency.[5,6] However, some of these processes are energy
38 and/or solvent-intensive, increasing the overall costs of the process while producing substantial
39 waste volumes.

40 Biosorption can be a sustainable and cost-effective approach for recovering metals from
41 wastewater.[7] Herein, biosorption is defined as the passive interaction of the biomass surface
42 with metal ions.. Biosorption can occur in living and non-living biomass. The use of non-living
43 biomass for metal sorption has several advantages such as good cost-effectiveness, application
44 in wider pH and metal concentration ranges, no need for additional nutrients and facilitated
45 metal recovery compared to intra-cellular metal accumulation.[8] Non-living biomass can afford
46 quicker and more efficient metal sorption than living biomass[9], also bearing advantages such
47 as control over proliferation and potential fouling events. The success of metal sorption depends
48 on the initial metal concentration, contact time, pH, metal:sorbent ratio and the presence of
49 competing ions.[10,11] Optimization of the sorption process also depends on understanding the
50 underlying mechanisms of metal sorption. Some of the mechanisms involved in metal sorption
51 include physical sorption, chemical sorption and ion-exchange.[12–14] The mechanism(s)
52 involved in metal sorption will also depend on the composition of the used biomass.

53 Several biomass matrices have been successfully employed for metal sorption, including fruit
54 waste,[15] nuts,[16] spent mushrooms,[11] coffee husk derivatives,[17] and seeds.[18]
55 Macroalgae, microalgae [19,20] and cyanobacteria[21] have also been widely studied for metal
56 sorption, due to their bioavailability, biodegradability, low-cost and efficiency.[9,22] The invasive

57 character of some algae also makes their removal environmentally beneficial. Metal sorption on
58 non-living organisms is related to their cell wall constitution. Metal interaction will mainly occur
59 *via* the functional groups present in the cell wall – carboxyl, hydroxyl, thiol, amino and phosphate
60 groups – and their abundance and availability will determine the success of biosorption.[23]
61 Efforts have been made to find effective biosorbents, with studies comparing the metal sorption
62 efficiency of different macroalgae[20,24,25] and, to a lesser extent, evaluating the efficiency of
63 macroalgae *vs* microalgae[26] and microalgae *vs* cyanobacteria.[27] Still, a simultaneous
64 comparison of macroalgae, microalgae and cyanobacteria under the same experimental
65 conditions seems to be lacking.

66 Algae and cyanobacteria are usually used for water decontamination in general rather than
67 specifically for metal recovery.[28] This causes some divergences in the optimization of metal
68 sorption. Water decontamination seeks the complete removal of metal from the wastewater,
69 often resulting in the addition of high biomass amounts for low metal concentrations.[19,29] In
70 contrast, using biosorption for metal recovery aims at the saturation of the functional groups of
71 the biomass, requiring a good equilibrium between biomass dosage and metal concentration to
72 ensure optimal metal pre-concentration. The selection of target metals and their concentration
73 also depends on the end goal. In water decontamination, it is common to study low metal
74 concentrations, sometimes close to the drinking water and wastewater limits,[30] with target
75 metals being selected due to their toxicity rather than their criticality and economical value.[31]
76 Studies using sorption for metal recovery tend to focus on aqueous solutions with higher metal
77 concentrations and rich in critical or valuable metals, such as acid mine drainage
78 wastewaters.[32] Overall, there is a lack of reports focusing on the use of algae and cyanobacteria
79 as metal pre-concentrators, but also a dearth of studies conducted on multi-elemental metal
80 solutions.[32,33] Most biosorption studies are based on aqueous solutions of a single metal,
81 disregarding the ion competition effect.[19,20,32,33] For metal recovery purposes, it is
82 important to consider metal competition since wastewaters are generally composed of several
83 metals.

84 Herein, a direct comparison of macroalgae, microalgae and cyanobacteria performance is
85 enabled while considering the metal competition effect. Eight algae (six macro- and two

86 microalgae) and three cyanobacteria were screened for metal sorption in multi-elemental
87 aqueous solutions. The metals Co^{2+} , Cu^{2+} , Ni^{2+} and Zn^{2+} were selected due to their significance for
88 developing low-carbon technology, criticality and their equal valency.[34–36] All biomass
89 samples were characterized through Fourier transform infrared (FTIR), elemental analysis and
90 total reflection X-ray fluorescence spectrometer (TXRF). The correlation between the biomass
91 composition (carbon, hydrogen, nitrogen, sulfur, oxygen, and ash content percents) and sorption
92 capacity was evaluated. The release of Ca^{2+} and K^{+} ions from the biomass to the aqueous solution
93 was studied to understand the underlying sorption mechanism better.

94 **2. Materials and Methods**

95 All chemicals were purchased and used as received. $\text{CoSO}_4 \cdot 7\text{H}_2\text{O}$ (> 99 wt %), $\text{CuSO}_4 \cdot 5\text{H}_2\text{O}$ (>
96 99 wt %) and $\text{ZnSO}_4 \cdot 7\text{H}_2\text{O}$ (> 99 wt %) were obtained from Merck. $\text{NiSO}_4 \cdot 6\text{H}_2\text{O}$ (> 99 wt %) was
97 purchased from Riedel de Haen. Yttrium standard ($1000 \text{ mg} \cdot \text{L}^{-1}$ of Y(III) in 2 wt % nitric acid),
98 poly(vinyl alcohol) (> 99 wt %) and Triton® X-100 (for analysis) were purchased from Sigma
99 Aldrich. All solutions were prepared in ultra-pure water which was obtained through a Millipore
100 filter system MilliQ®. All metal solutions were prepared by gravimetrically weighing ($\pm 10^{-4}$ g) the
101 correct amount of each metal salt. The glass material was previously washed with nitric acid (20
102 v/v %) purchased from Merck (65 wt %) and further rinsed with ultra-pure water.

103 **2.1. Biomass collection and pre-treatment**

104 Six macroalgae (*Gracilaria sp.*, *Gelidium sp.*, *Sargassum sp.*, *Saccharina latissima*, *Ulva rigida*
105 *and Undaria pinnatifida*), two microalgae (*Isochrysis galbana* and *Phaeodactylum tricornutum*)
106 and three cyanobacteria (*Anabaena cylindrica* PCC 7122, *Nostoc muscorum* UTAD_N213 and
107 *Spirulina sp.*) were screened for their metal sorption capacity. *U. rigida*, *Gracilaria sp.*, *U.*
108 *pinnatifida*, *Sargassum sp.* and *Gelidium sp.* were kindly provided by ALGApplus, Lda. *Gracilaria*
109 *sp.* was received dry and ground while *U. rigida*, *U. pinnatifida* and *Sargassum sp.* were also
110 received dry, but grinding was performed in the laboratory by freezing the biomass with liquid
111 nitrogen and immediately grinding it with a domestic coffee grinder. The obtained particles were
112 mechanically sieved to select particles with a size under 200 μm . *S. latissima* was kindly provided
113 by Algaia SA (Saint Lô, France). *S. latissima* and *Gelidium sp.* were pre-dried before delivery and

114 ground at lab scale as previously described. *I. galbana* and *P. tricornutum* were acquired dry at
115 Necton S.A. and used without further treatment. *Spirulina sp.* was purchased dry from Shine
116 Superfoods – Alma & Valor and used as received. *A. cylindrica* PCC 7122 and *N. muscorum*
117 UTAD_N213 were cultured in 5 L Schott Duran® glassware containing sterilized liquid Woods Hole
118 culture medium (MBL),[37] in an incubation chamber at (293 ± 2) K, under a 16:8 h light-dark
119 photoperiod using 2300 lx from cool white fluorescent tubes. After 13 days in culture, the
120 biomass was harvested and concentrated through centrifugation at 277 K and 4111 g. The fresh
121 biomass was freeze-dried at < 150 mTorr resorting to a benchtop K, VirTis with a Vacuumbrand
122 pump for one week. All biomass was kept in a dry and light-protected place at room temperature.

123 **2.2. Biosorption batch studies**

124 Since this work is focused on metal recovery, a fair metal:biomass ratio is required to achieve
125 good metal pre-concentration. In mono-metallic assays with Cu^{2+} , Ni^{2+} and Zn^{2+} , promising results
126 were achieved with an initial metal concentration of 50 ppm and 500 ppm of non-living algae.[20]
127 Since in multi-elemental assays the metal sorption efficiency is deemed to be lower than in mono-
128 elemental assays, herein the total initial metal concentration was reduced to 40 ppm, with 10
129 ppm each of Cu^{2+} , Co^{2+} , Ni^{2+} and Zn^{2+} being simultaneously placed in contact with 500 ppm of
130 algae. The pH of the solutions was adjusted to 4 by adding diluted sulfuric acid and determined
131 using a Mettler Toledo SevenMultiTMdual pH meter (± 0.02). At low pH values, there is
132 competition between protons and metals for the available binding sites, which limits the metal
133 sorption efficiency of the biomass.[38] In contrast, at high pH values, metal precipitation may
134 occur, once again hindering the metal sorption efficiency. Thus, performing the screening assay
135 at pH = 4 is a reasonable compromise. The batch experiments were conducted in Schott Duran®
136 glassware in an orbital shaker (IKA KS4000 ic control) at 200 rpm and (303 ± 1) K by adding 500
137 ppm of dried non-living biomass to each multi-elemental metal solution (100 mL). No biomass
138 was added to the control which was simultaneously subjected to the same procedure as the
139 samples. No metal loss was verified in the controls over time. Samples of sorbent suspension
140 were collected (1.5 mL) after 6 and 24 h of contact, centrifuged for 2 min at 12000 rpm and the
141 liquid phase was separated from the residual biomass. All assays were conducted in triplicate.

142 2.3. Metal quantification

143 Metal quantification was performed by total reflection X-ray fluorescence spectrometry
144 (TXRF) using a Picofox S2 (Bruker Nano (Billerica, MA, USA)) equipped with a molybdenum X-ray
145 source. All the analyses were conducted at a 50 kV voltage and 600 μ A current for 300 seconds.
146 Quartz sample carriers were coated with 10 μ L of silicon in isopropanol solution and dried at (353
147 \pm 1) K for at least 15 min. A known amount of yttrium was added to each sample and 10 μ L of
148 this solution was added to a pre-treated quartz carrier and dried at (353 \pm 1) K for at least 30 min.

149 The amount of metal *per* unit of biomass (sorption capacity, q , $\text{mmol}\cdot\text{g}^{-1}$) at time t was
150 calculated according to Equation 1:

$$151 \quad q = \frac{V (C_0 - C_t)}{m} \quad 1$$

152 where V is the volume of the solution (L), C_0 ($\text{mmol}\cdot\text{L}^{-1}$) is the initial concentration of each metal,
153 C_t ($\text{mmol}\cdot\text{L}^{-1}$) is the concentration of each metal at that time (t) and m is the biomass mass (g).
154 The selectivity of the biomass was determined as shown in Equation 2:

$$155 \quad S = \frac{q_{\text{metal1}}}{q_{\text{metal2}}} \quad 2$$

156 where q_{metal1} ($\text{mmol}\cdot\text{g}^{-1}$) is the sorption capacity of a metal and q_{metal2} ($\text{mmol}\cdot\text{g}^{-1}$) is the sorption
157 capacity of a second metal.

158 2.4. Biomass characterization

159 All the evaluated non-living biomass matrices were characterized via Fourier transform
160 infrared (FTIR), elemental analysis and total reflection X-ray fluorescence spectrometry (TXRF).
161 The FTIR spectra of biomass samples were acquired by a PerkinElmer Spectrum BX spectrometer
162 with a diamond crystal and a horizontal Golden Gate attenuated total reflection (ATR) cell. Each
163 sample was analyzed at wavenumbers ranging from 4000 to 400 cm^{-1} , with a resolution of 4 cm^{-1}
164 and a total of 32 scans. While the FTIR of the biomass pre-sorption was acquired for all biomass
165 samples the spectra after sorption were only acquired for the macroalgal *Sargassum sp.*, the
166 microalgal *P. tricornutum*) and the cyanobacterium (*Spirulina sp.*). The elemental analysis (C, H,
167 N and S) of the biomass samples was obtained using the equipment LECO TruSpec series 630-

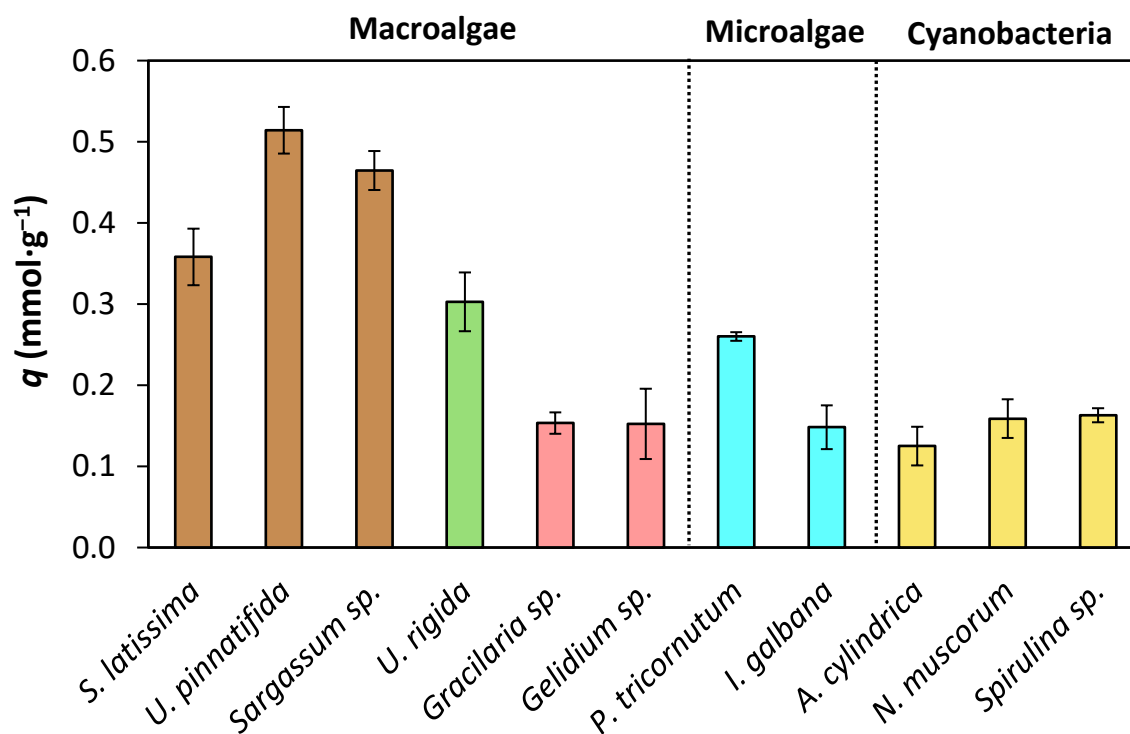
168 200-200 (Michigan, US), whereas the oxygen content was determined by difference after ash
169 content determination. The calcium and potassium content of all biomass matrices was
170 evaluated via TXRF by suspending the biomass in a solution of 0.8 g of poly(vinyl alcohol) (1 wt
171 %) and 0.2 g of Triton® X-100 (1 wt %), spiked with a known concentration of yttrium. The
172 subsequent sample preparation was made as described in sub-section 2.3.

173 **3. Results and Discussion**

174 The biomass screening included different macroalgae, microalgae and cyanobacteria to
175 facilitate the simultaneous comparison of the metal sorption capacity of different biomass. This
176 is usually done by comparing works conducted under different experimental conditions [20] and
177 limited biomass diversity,[19,39] which hinders the comparison of the sorption capacity of
178 macroalgae, microalgae and cyanobacteria.[19,20,39,40] A comprehensive screening was
179 performed in multi-elemental metal solutions since metal recovery often involves complex
180 matrices. All biomass samples were analyzed by elemental analysis and FTIR to better understand
181 their composition. The presence of inorganic elements in the biomass structure was evaluated
182 by TXRF. The release of ions such as Ca^{2+} and K^+ during the sorption process was evaluated to
183 better understand the mechanism behind metal sorption in the different biomass samples.

184 **3.1. Screening assay**

185 To evaluate the potential of different algal biomass samples for metal sorption, eleven
186 samples were selected and placed in contact with a multi-elemental solution of Co^{2+} , Cu^{2+} , Ni^{2+}
187 and Zn^{2+} , each with a concentration of 10 ppm and at pH = 4. After placing the biomass in contact
188 with the metal solution, samples were collected at 6 and 24 h. No significant differences in the
189 sorption capacity of the biomass were found across time (Figure S1). The sorption capacity of
190 each biomass after 6 h of contact is represented in Figure 1.

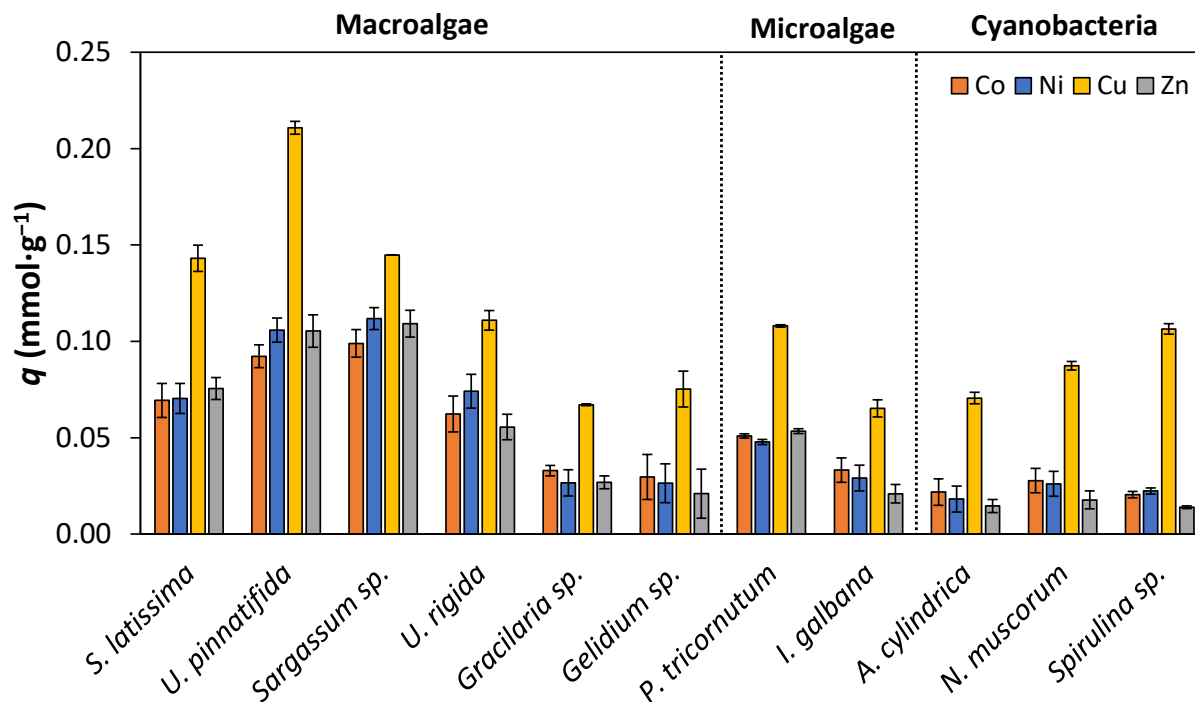


191
 192 **Figure 1.** Metal sorption capacity (q , mmol·g⁻¹) of each biomass at a total metal concentration of
 193 40 ppm, 500 ppm of biomass, $T = (303 \pm 1)$ K, pH = 4 and $t = 6$ h. Colors were used to differentiate
 194 the biomass samples: brown bars for brown macroalgae, green bars for green macroalgae, pink
 195 bars for red macroalgae, blue bars for microalgae and yellow bars for cyanobacteria.

196 Brown macroalgae afforded better metal sorption capacity values than the remaining biomass
 197 types, followed by the green macroalgae *U. rigida*. The red macroalgae showed the lowest
 198 sorption capacity within the macroalgae group. Similar tendencies were previously reported in
 199 mono-elemental sorption studies, with brown macroalgae being a more promising metal sorbent
 200 than green and red macroalgae.[24,25] Brown macroalgae are rich in alginic acid and, therefore,
 201 display a large number of carboxyl and hydroxyl groups.[41] This may justify their higher ability
 202 for metal sorption, especially at pH values close to the acid dissociation constant of carboxylic
 203 acids (pK_a 1.7 – 4.7).[41,42] Sheng *et al.*[43] reported mono-elemental studies using dried non-
 204 living *Sargassum sp.*, *Ulva sp.* and *Gracilaria sp.* for the sorption of Cu^{2+} , Ni^{2+} and Zn^{2+} . Overall,
 205 the metal sorption trend was the same as observed here: *Sargassum sp.* > *Ulva sp.* > *Gracilaria*
 206 *sp.* The maximum sorption capacity obtained in this mono-elemental assay is significantly higher

207 than those obtained here. This highlights that the presence of multiple ions in solution promotes
208 intra-system competition and lowers the sorption capacity. Hence, mono-elemental studies do
209 not reflect the real biomass potential for metal sorption in more complex matrices, as
210 wastewaters. As for microalgae, *P. tricornutum* afforded more promising results than *I. galbana*,
211 with its total sorption capacity being similar to that of the green macroalgal *U. rigida*. To the best
212 of our knowledge, there are no reports employing the non-living *P. tricornutum* and *I. galbana*
213 for metal sorption in either mono- or multi-elemental studies. The different sorption capacity of
214 these two microalgae may rely on their structural differences. *P. tricornutum* is a diatom and,
215 therefore, has a silica frustule rich in silanol groups, hydroxyl and carboxyl groups.[44] Although
216 no silanol groups were identified in the FTIR spectrum of *P. tricornutum*, its corresponding peaks
217 may be overlapping with other functional groups. Regarding cyanobacteria, their sorption
218 capacity was comparable to that of the red macroalgae and the microalgae *I. galbana*. Mono-
219 elemental studies involving *Anabaena sp.*, *Nostoc sp.* and *Spirulina platensis*. [45,46] afforded
220 higher sorption capacity values than those obtained herein. Overall, our results reinforce the
221 need to evolve from mono- to multi-elemental studies and enable the establishment of a trend
222 for the biomass sorption capacity that seems to be as follows: cyanobacteria < microalgae <
223 macroalgae.

224 Despite having different metal sorption capacities, all the evaluated biomass samples display
225 a selective metal sorption behavior, as depicted in Figure 2.



226
 227 **Figure 2.** Metal sorption capacity (q , $\text{mmol}\cdot\text{g}^{-1}$) of each biomass for Co^{2+} (orange bars), Ni^{2+} (blue
 228 bars), Cu^{2+} (yellow bars) and Zn^{2+} (grey bars).

229 All the studied biomass samples showed a higher affinity for Cu^{2+} than for the remaining metals.
 230 No other consistent sorption pattern could be identified across all the biomass samples for Co^{2+} ,
 231 Ni^{2+} and Zn^{2+} . Although cyanobacteria were the least effective biosorbent, they displayed the
 232 highest relative Cu^{2+} selectivity (see Figure S2). The affinity for Cu^{2+} is likely related to the
 233 complexation constant of these metals with the functional groups relevant to sorption. For
 234 instance, in the case of a simple carboxylic acid like acetic acid, the logarithm of the complexation
 235 constant values for each metal at 298 K and 0 ionic strength is as follows: 1.5 Co^{2+} , 2.2 Cu^{2+} , 1.4
 236 Ni^{2+} and 1.6 Zn^{2+} (see Table S1).[47] The metal ion Cu^{2+} presents a higher complexation constant
 237 value than the remaining evaluated metals and, as a consequence, it is preferentially sorbed. The
 238 remaining metals share similar complexation constants, which leads to their indiscriminate
 239 sorption onto the biomass. The greater complexation constant value of Cu^{2+} , in comparison to
 240 Co^{2+} , Ni^{2+} and Zn^{2+} , is also verified for the hydroxide ion[48] and most amino acids.[49] The
 241 preferential removal of Cu^{2+} over Co^{2+} , Ni^{2+} and Zn^{2+} was reported in other studies,[20,43]
 242 including in multi-elemental sorption assays performed in acid mine drainage wastewaters.[32]

243 The Cu^{2+} selectivity is also in agreement with the Irving-Williams series.[50,51] The Irving-
244 Williams series describes the relative stability order of octahedral complexes formed by M^{2+} first-
245 row transition metal, irrespective of the ligand. The stability order of these complexes for the
246 replacement of water by other ligands is as follows: $\text{Mn}^{2+} < \text{Fe}^{2+} < \text{Co}^{2+} < \text{Ni}^{2+} < \text{Cu}^{2+} > \text{Zn}^{2+}$. [50,51]
247 These findings are mainly related to the ionic radius of the elements and the crystal field
248 stabilization energy. The higher stability of the octahedral Cu^{2+} complex represents an exception
249 to this due to the Jahn–Teller effect. Briefly, in the case of Cu^{2+} , there is an uneven distribution
250 of electrons in the e_g set of orbitals, enabling the possibility to asymmetrically fill the orbitals.
251 This is followed by Jahn–Teller distortion, which causes a tetragonal elongation and the
252 stabilization of the complex.[52] This comparison is facilitated due to the uniform valency of the
253 studied metals (M^{2+}). Sorption assays involving metals with different valency will probably impact
254 the trends presented in this work.

255 **3.2. Biomass characterization and sorption mechanism**

256 The carbon, hydrogen, nitrogen, sulfur, oxygen, ash content (%) and carbon/oxygen ratio (C/O)
257 of the screened biomass is presented in Table 1.

258

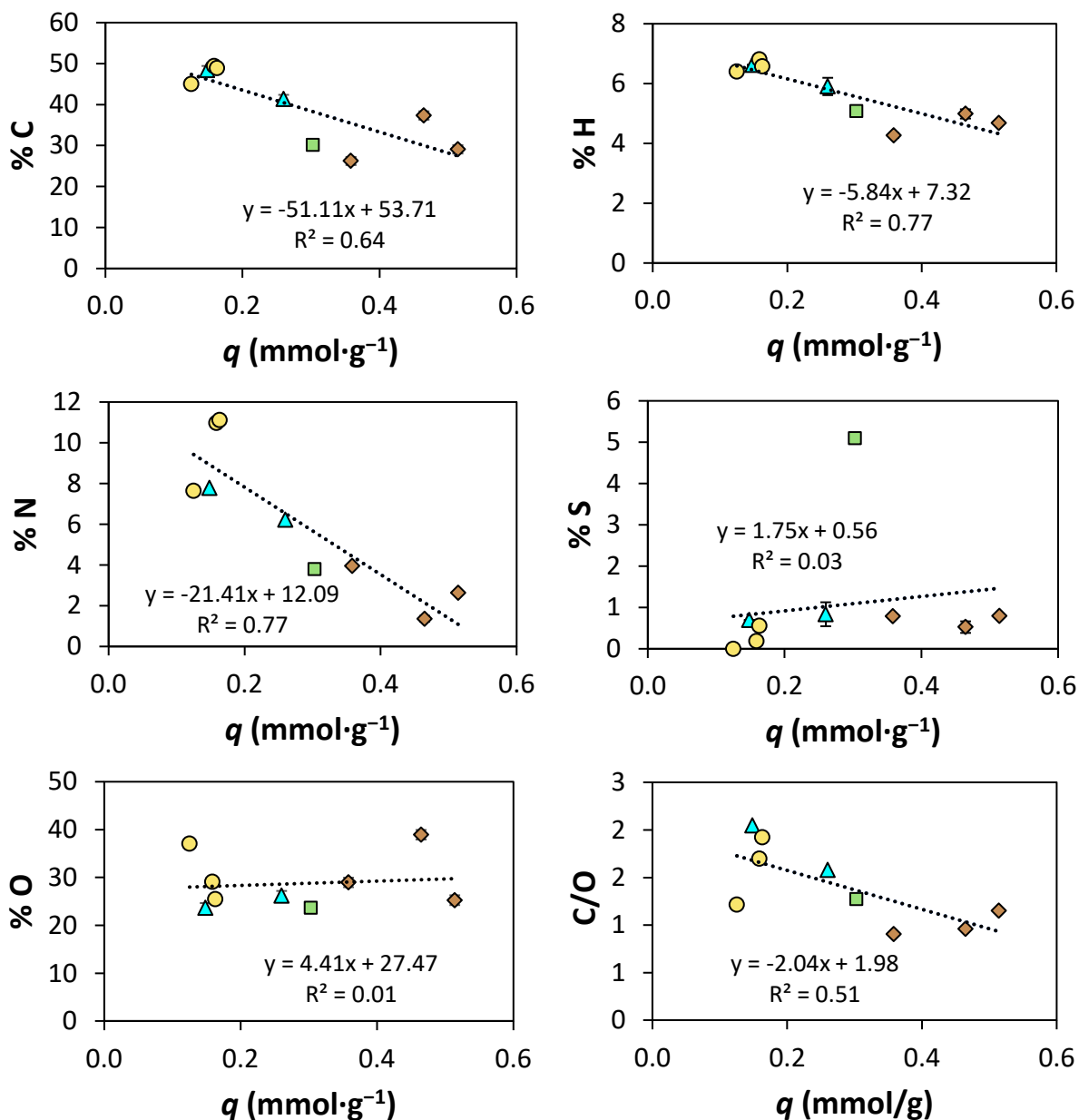
259 **Table 1.** Carbon, hydrogen, nitrogen, sulfur, oxygen, ash content (%) and C/O ratio of the non-
 260 living dry biomass.

	Biomass	% C $\pm \sigma$	% H $\pm \sigma$	% N $\pm \sigma$	% S $\pm \sigma$	% ash	% O	C/O ratio
Macroalgae	<i>S. latissima</i>	26.2 \pm 0.1	4.3 \pm 0.1	3.94 \pm 0.04	0.8 \pm 0.4	36	29	0.9
	<i>U. pinnatifida</i>	29.1 \pm 0.1	4.68 \pm 0.02	2.63 \pm 0.03	0.8 \pm 0.4	37	25	1.1
	<i>Sargassum sp.</i>	37.3 \pm 0.2	5.0 \pm 0.1	1.3 \pm 0.1	0.5 \pm 0.1	17	39	1.0
	<i>U. rigida</i>	30.10 \pm 0.01	5.1 \pm 0.1	3.78 \pm 0.08	5.1 \pm 0.7	32	24	1.3
	<i>Gracilaria sp.</i>	32.9 \pm 0.2	4.92 \pm 0.08	3.41 \pm 0.07	2.0 \pm 0.1	27	30	1.1
	<i>Gelidium sp.</i>	38.3 \pm 0.1	5.85 \pm 0.06	3.06 \pm 0.07	1.9 \pm 0.3	16	35	1.1
Microalgae	<i>P. tricornutum</i>	41.3 \pm 0.2	5.9 \pm 0.2	6.22 \pm 0.04	0.8 \pm 0.2	19	26	1.6
	<i>I. galbana</i>	48.42 \pm 0.03	6.63 \pm 0.06	7.770 \pm 0.004	0.7 \pm 0.1	13	24	2.0
Cyanobacteria	<i>A. cylindrica</i>	45.0 \pm 0.2	6.4 \pm 0.3	7.64 \pm 0.04	0 \pm 0	4	37	1.2
	<i>N. muscorum</i>	49.4 \pm 0.1	6.81 \pm 0.01	10.97 \pm 0.05	0.19 \pm 0.03	3	29	1.7
	<i>Spirulina sp.</i>	48.9 \pm 0.4	6.57 \pm 0.07	11.1 \pm 0.3	0.55 \pm 0.04	7	25	1.9

261 Overall, all biomass samples display high carbon and oxygen content but low hydrogen, nitrogen
 262 and sulfur percent. The ash content ranged from 3 to 37 % with macroalgae generally having a
 263 higher ash percent than microalgae and cyanobacteria. Macroalgae exhibited low nitrogen
 264 content, which could be a reflection of their overall poor protein content, as reported
 265 elsewhere.[53] In addition, macroalgae display lower C/O ratio values than microalgae and
 266 cyanobacteria. Brown macroalgae (*S. latissima*, *U. pinnatifida* and *Sargassum sp.*) afforded the
 267 lowest C/O ratio values, which can be linked to their high alginic acid content and low lipid
 268 abundance. [41,53] Both the green (*U. rigida*) and red macroalgae (*Gracilaria sp.* and *Gelidium*
 269 *sp.*) have higher sulfur content than the remaining samples. In the case of the red macroalgae,
 270 this is likely related to the abundance of sulfated galactan in their structure.

271 The biomass elemental composition was plotted against its sorption capacity (q , mmol·g⁻¹)
 272 to study a potential correlation between these parameters (Figure 3). Red macroalgae (*Gracilaria*

273 *sp.* and *Gelidium sp.*) were excluded from this evaluation as they do not follow the trends
 274 observed for the other biomass samples.



275
 276 **Figure 3.** Correlation between carbon, hydrogen, nitrogen, sulfur, oxygen, ash content (%) and
 277 carbon/oxygen ratio with the sorption capacity (q , $\text{mmol}\cdot\text{g}^{-1}$) of the screened biomass. Each color
 278 represents a set of organisms, brown (\diamond) corresponding to brown macroalgae, green (\square) to green
 279 macroalgae, blue (Δ) to microalgae and yellow (\circ) to cyanobacteria.

280 The data suggest a strong correlation between carbon, nitrogen and hydrogen content and the
 281 metal sorption capacity. On the other hand, the sulfur and oxygen biomass content do not seem
 282 to be associated with the sorption capacity of the biomass. The plot of C/O ratio *versus* metal
 283 sorption capacity seems to suggest that higher C/O ratios are linked to lower sorption capacity
 284 values. Still, this dependency is weak and more data would be required to validate this
 285 observation. In this work ground non-living biomass was used in all assays. For this reason, there
 286 is no distinction between intracellular or surface groups, with all functional groups being available
 287 to interact with metal. Establishing these correlations in living biomass is not valid since not all
 288 elements will be available for metal interaction, depending on their location.

289 The sorption of metals highly depends on the functional groups present in each biomass
 290 sample. FTIR was used to identify the main functional groups of each biomass and details are
 291 presented in Tables 2 and 3. Spectra details can be consulted in Figure S3 and S4.

292 **Table 2.** Identification of the main FTIR bands of the studied macroalgae before metal sorption.

Band origin	Wavenumber (cm ⁻¹)					
	<i>S. latissima</i>	<i>U. pinnatifida</i>	<i>Sargassum sp.</i>	<i>U. rigida</i>	<i>Gracilaria sp.</i>	<i>Gelidium sp.</i>
v O–H (polysaccharides), v N–H (proteins)	3269	3285	3278	3208	3296	3354
v C–H of aliphatic groups	2934	2925	2925	2950	2924, 2871	2927
v C=O (amide I band)	1633	1622	1610	1633	1644	1633
δ N–H (amide II band)	1538	1538	1542	1548	1538	1548
δ O–H (carboxyl and hydroxyl groups)	1416	1416	1420	1404	1416	1415
δ C–H, δ O–H, (III amide band, proteins)	–	1241	1213	1227	–	–
v C–O (aliphatic ether, primary and secondary alcohol)	1081, 1021	1028	1161, 1028	1149, 1082	1035	1149, 1035
v C–O	931	–	–	–	930	931

293

294 **Table 3.** Identification of the main FTIR bands of the studied microalgae and cyanobacteria before
 295 metal sorption.

Band origin	Wavenumber (cm ⁻¹)				
	Microalgae		Cyanobacteria		
	<i>P. tricornutum</i>	<i>I. galbana</i>	<i>A. cylindrica</i>	<i>N. muscorum</i>	<i>Spirulina sp.</i>
v O–H (polysaccharides), v N–H (proteins)	3280	3274	3280	3282	3280
v C–H of aliphatic groups	2959, 2923, 2852	2957, 2919, 2849	2957, 2926, 2894, 2856	2923, 2875, 2852	2926, 2874, 2856
v C=O (amide I band)	1633	1633	1644	1634	1634
δ N–H (amide II band)	1538	1538	1538	1538	1538
δ C–H (methyl and methylene groups)	1469	1454	1454	1454	1454
δ O–H (carboxyl and hydroxyl groups)	1402	1403	1393	1393	1393
δ C–H, δ O–H, (III amide band, proteins)	1227	1234	1241	1240	1239
v C–O (aliphatic ether, primary and secondary alcohol)	1039	1103, 1072, 1040	1151, 1078, 1022	1152, 1045	1030

296

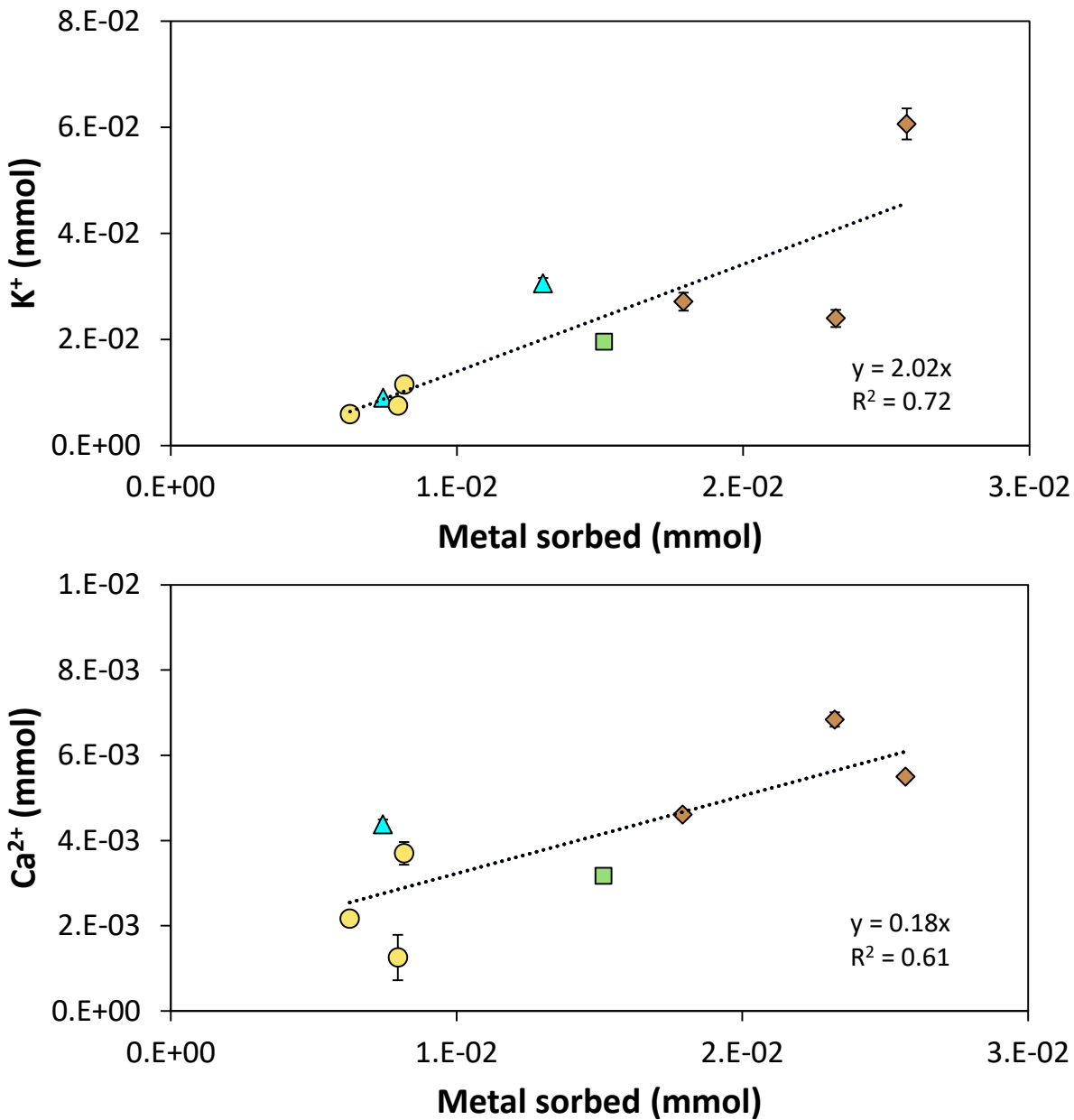
297 According to the FTIR spectra, all the evaluated biomass samples presented O–H and N–H
 298 stretching vibrations around 3208 and 3296 cm⁻¹, C=O stretching vibration from the amide I band
 299 at 1610–1644 cm⁻¹ and N–H stretching vibration of the amide II band at 1538–1542 cm⁻¹. The
 300 FTIR spectra of *Sargassum sp.* showed some changes after contact with the multi-elemental
 301 metal solution. For instance, the peak at 1321 cm⁻¹ corresponding to the C–O stretching vibration
 302 disappeared upon contact with the metal solution. There are also modifications around 1416 cm⁻¹
 303 ¹, suggesting the involvement of carboxyl groups. In the case of *P. tricornutum*, there are
 304 modifications in the amide II band region (≈ 1542 cm⁻¹), corresponding to N–H bending
 305 vibrations. This macroalgae also presents modifications around 1402 cm⁻¹, corresponding to
 306 carboxyl and hydroxyl bending vibrations and modifications around 1469 cm⁻¹ corresponding to
 307 methyl and methylene bending vibrations. *Spirulina sp.* showed no significant alterations before
 308 and after metal sorption. Among these three biomass samples, *Spirulina sp.* was the least
 309 efficient metal sorbent. The amount of metal sorbed to its cell wall may not be enough to afford

310 visible changes in the FTIR analysis. Of the identified functional groups, the carboxyl groups seem
311 to be significantly involved in metal sorption. At pH = 4 most carboxyl groups are deprotonated
312 (pK_a 1.7 – 4.7) and, therefore, available for metal sorption.[42] Despite the importance of the
313 carboxyl groups for metal sorption, according to the oxygen percent and sorption capacity
314 correlation, the oxygen content alone does not seem to be directly related to the sorption
315 capacity of the biomass, as shown in Figure 1. In this case, the availability of the right type of
316 oxygen-containing functional groups to interact with metals may be more important than their
317 abundance.

318 Since ion-exchange is one of the potential mechanisms behind metal sorption,[54] the
319 inorganic components of the biomass samples were quantified *via* TXRF and are presented in
320 Table S2. The evaluated biomass samples have significant concentrations of Cl^- , K^+ and Ca^{2+}
321 (Figure S5). TXRF is not the most suitable equipment for anion quantification so the presented
322 Cl^- concentration may not be accurate. The abundance of K^+ and Ca^{2+} is particularly relevant from
323 an ion-exchange point of view. Other ions such as Na^+ and Mg^{2+} are also expected to be in the
324 biomass structure but their quantification is not feasible in TXRF. These ions are generally
325 coordinated with the acidic functional groups of the biomass and can be exchanged by other
326 cations present in the solution. The abundance and diversity of ions in the biomass structure are
327 influenced by the environment where they are grown. For instance, the lab-grown cyanobacteria
328 *A. cylindrica* and *N. muscorum* may display significantly lower amounts of these inorganic ions
329 due to the controlled environment they were grown in. No obvious correlation was found
330 between the K^+ and Ca^{2+} concentration on the biomass and its sorption capacity.

331 Considering that, as discussed above, some metal complexes are more stable than others, it
332 is likely that under appropriate conditions a metal can displace another ion from a less stable
333 complex.[50] To better understand the sorption mechanism, besides the Ca^{2+} and K^+
334 concentrations present on the biomass samples detailed in Table S2, the Ca^{2+} and K^+
335 concentrations were measured for all the controls and samples. While the controls showed no
336 traces of these ions, a significant release of Ca^{2+} and K^+ from the biomass to the multi-elemental
337 metal solution was observed in all biomass samples upon metal sorption. The release of these
338 ions was quantified *via* TXRF for all assays and is depicted in Figure S6. The correlation between

339 the release of Ca^{2+} and K^+ ions and metal sorption is presented in Figure 4. As in the elemental
340 composition vs q correlation, red macroalgae (*Gracilaria sp.* and *Gelidium sp.*) were excluded
341 from the analyses as they have a behavior clearly different from the other biomass samples
342 studied. The cyanobacterium *P. tricornutum* was also excluded, but only from the Ca^{2+} release vs
343 q correlation, as it significantly impaired the trend (R^2 drop from 0.61 to 0.11).
344



345

346 **Figure 4.** Correlation of the K^+ and Ca^{2+} release with the metal sorbed (mmol) for the different
347 biomass samples. Colors were used to differentiate the biomass: brown (\diamond) for brown
348 macroalgae, green (\square) for green macroalgae, blue (Δ) for microalgae and yellow (\circ) for
349 cyanobacteria. The linear regression is represented by the black dotted line.

350 The K^+ release seem to be linked to a large extent to the metal loading into the biomass with 2
351 ions being removed to allow the sorption of a metal ion, as would be expected from the
352 electroneutrality. Although much weaker, the release of Ca^{2+} also seems to contribute to the
353 metal sorption. The total amount of released K^+ and Ca^{2+} was charge normalized and compared
354 to the amount of sorbed metals (see Figure S7). Overall, the amount of released ions is very
355 similar to the amount of sorbed metals when considering charge normalization. The only
356 exception is *U. pinnatifida*, where the sum of normalized K^+ and Ca^{2+} exceeds the amount of
357 sorbed metals. Since K^+ and Ca^{2+} largely account for all sorbed metals, other ions as Mg^{2+} and Na^+
358 are unlikely to be involved in the described sorption mechanism. The displacement of these ions
359 confirms the involvement of the ion-exchange mechanism in multi-elemental metal sorption
360 assays. The replacement of the Ca^{2+} and K^+ ions can be further related to their complexation
361 constants with the biomass functional groups. According to the complexation constant values of
362 Ca^{2+} , K^+ , Co^{2+} , Cu^{2+} , Ni^{2+} and Zn^{2+} with the hydroxide ion and carboxylic acids (oxalic and citric
363 acid),[47,48] Ca^{2+} and K^+ typically have lower complexation constants than the evaluated
364 transition metals. In the case of the hydroxide ion, the logarithm of the complexation constant
365 values for each metal at 298 K and 0 ionic strength is as follows: 1.3 Ca^{2+} , -0.5 K^+ , 4.3 Co^{2+} , 6.3
366 Cu^{2+} , 4.1 Ni^{2+} and 5.0 Zn^{2+} (Table S1). When compared to Ca^{2+} , K^+ has a lower complexation
367 constant. Consequently, K^+ should be more easily exchanged with metal ions than Ca^{2+} . This is
368 supported by the obtained data since K^+ ions were more extensively released from the biomass
369 to the aqueous solution than Ca^{2+} ions (see Figure 4). The red algae always diverge from the
370 presented correlations, suggesting that their metal sorption mechanism may differ from that
371 described for the remaining biomass samples.

372 **4. Conclusions**

373 Eleven non-living algal biomass samples were screened for metal sorption in multi-elemental
374 metal solutions containing equal concentrations of Co^{2+} , Cu^{2+} , Ni^{2+} and Zn^{2+} at (303 ± 1) K and pH
375 = 4. The composition of the biomass was found to be correlated with their sorption capacity.
376 According to the FTIR spectra of the biomass, carboxyl groups are involved in metal sorption.
377 Despite the strong involvement of oxygen-rich groups in metal sorption, higher biomass oxygen
378 contents do not correlate with better metal sorption capacity values, suggesting that the type,
379 distribution and accessibility of the functional groups are more important than their abundance.
380 Brown macroalgae afforded higher metal sorption capacity values than the remaining evaluated
381 biomass samples. Regardless of being macroalgae, microalgae or cyanobacteria, all biomasses
382 showed a higher affinity for Cu^{2+} sorption. To shed light on the metal sorption mechanism in
383 multi-elemental assays, the release of Ca^{2+} and K^+ to the aqueous media was investigated. The
384 obtained results suggest that the release of these ions, in particular K^+ , is linked to the metal
385 sorption capacity values. This indicates that for most of the studied biomass types, ion-exchange
386 is the prevalent mechanism involved in metal sorption. Altogether, using biomass as a pre-
387 concentrator can be a viable vessel for metal recovery from multi-elemental metal solutions.

388 **Acknowledgments**

389 This work was developed within the scope of the project CICECO-Aveiro Institute of
390 Materials, UIDB/50011/2020, UIDP/50011/2020 & LA/P/0006/2020, financed by national funds
391 through the FCT/MEC (PIDDAC) and CESAM (UIDP/50017/2020 + UIDB/50017/2020 +
392 LA/P/0094/2020). Ana R. F. Carreira, Telma Veloso and Inês P. E. Macário acknowledge FCT for
393 the Ph.D. grants SFRH/BD/143612/2019, SFRH/BD/147346/2019 and SFRH/BD/123850/2016,
394 respectively. Helena Passos acknowledges FCT – Fundação para a Ciência e a Tecnologia, I.P. for
395 the researcher contract CEECIND/00831/2017 under the Scientific Employment Stimulus -
396 Individual Call 2017. The authors acknowledge the financial support of FCT regarding the project
397 REFINECYANO (PTDC/BTA-BTA/30914/2017). The authors would like to thank Nicolas Schaeffer
398 (CICECO) for fruitful discussions and ALGAplus, Lda. for providing algal samples.

399 **Conflicts of interest:** The authors declare no conflicts of interest.

400

401 **References**

- 402 [1] P. Li, M. feng CAI, Challenges and new insights for exploitation of deep underground
403 metal mineral resources, *Trans. Nonferrous Met. Soc. China (English Ed.* 31 (2021) 3478–
404 3505. [https://doi.org/10.1016/S1003-6326\(21\)65744-8](https://doi.org/10.1016/S1003-6326(21)65744-8).
- 405 [2] A. Nobahar, A.B. Melka, A. Pusta, J.P. Lourenço, J.D. Carlier, M.C. Costa, A New
406 Application of Solvent Extraction to Separate Copper from Extreme Acid Mine Drainage
407 Producing Solutions for Electrochemical and Biological Recovery Processes, *Mine Water*
408 *Environ.* 41 (2022) 387–401. <https://doi.org/10.1007/S10230-022-00858-7/FIGURES/9>.
- 409 [3] R. Millán-Becerro, F. Macías, C.R. Cánovas, R. Pérez-López, J.M. Fuentes-López,
410 Environmental management and potential valorization of wastes generated in passive
411 treatments of fertilizer industry effluents, *Chemosphere.* 295 (2022) 133876.
412 <https://doi.org/10.1016/j.chemosphere.2022.133876>.
- 413 [4] D. Dutta, S. Arya, S. Kumar, Industrial wastewater treatment: Current trends,
414 bottlenecks, and best practices, *Chemosphere.* 285 (2021) 131245.
415 <https://doi.org/10.1016/j.chemosphere.2021.131245>.
- 416 [5] T. Dolker, D. Pant, Chemical-biological hybrid systems for the metal recovery from waste
417 lithium ion battery, *J. Environ. Manage.* 248 (2019) 109270.
418 <https://doi.org/10.1016/j.jenvman.2019.109270>.
- 419 [6] I. Birloaga, F. Vegliò, An innovative hybrid hydrometallurgical approach for precious
420 metals recovery from secondary resources, *J. Environ. Manage.* 307 (2022) 114567.
421 <https://doi.org/10.1016/j.jenvman.2022.114567>.
- 422 [7] G. Dodbiba, J. Ponou, T. Fujita, Biosorption of heavy metals, in: *Microbiol. Miner. Met.*
423 *Mater. Environ.*, 2015: pp. 409–426. <https://doi.org/10.4018/978-1-5225-8903-7.ch077>.
- 424 [8] K.A. Salam, Towards sustainable development of microalgal biosorption for treating
425 effluents containing heavy metals, *Biofuel Res. J.* 6 (2019) 948–961.
426 <https://doi.org/10.18331/BRJ2019.6.2.2>.

- 427 [9] Z. Lin, J. Li, Y. Luan, W. Dai, Application of algae for heavy metal adsorption: A 20-year
428 meta-analysis, *Ecotoxicol. Environ. Saf.* 190 (2020) 110089.
429 <https://doi.org/10.1016/j.ecoenv.2019.110089>.
- 430 [10] A.E.S.M. Shaaban, R.K. Badawy, H.A. Mansour, M.E. Abdel-Rahman, Y.I.E. Aboulsoud,
431 Competitive algal biosorption of Al³⁺, Fe³⁺, and Zn²⁺ and treatment application of some
432 industrial effluents from Borg El-Arab region, Egypt, *J. Appl. Phycol.* 29 (2017) 3221–
433 3234. <https://doi.org/10.1007/s10811-017-1185-4>.
- 434 [11] A.N. Kamarudzaman, S.N. Ain Che Adan, Z. Hassan, M. Ab Wahab, S.M. Zaini Makhtar,
435 N.A. Abu Seman, M.F. Ab Jalil, D. Handayani, A. Syafiuddin, Biosorption of copper(II) and
436 iron(II) using spent mushroom compost as biosorbent, *Biointerface Res. Appl. Chem.* 12
437 (2022) 7775–7786. <https://doi.org/10.33263/BRIAC126.77757786>.
- 438 [12] C. Escudero-Oñate, I. Villaescusa, The Thermodynamics of Heavy Metal Sorption onto
439 Lignocellulosic Biomass, *Heavy Met.* (2018). <https://doi.org/10.5772/intechopen.74260>.
- 440 [13] K.G. Akpomie, F.A. Dawodu, K.O. Adebowale, Mechanism on the sorption of heavy
441 metals from binary-solution by a low cost montmorillonite and its desorption potential,
442 *Alexandria Eng. J.* 54 (2015) 757–767. <https://doi.org/10.1016/j.aej.2015.03.025>.
- 443 [14] V. Javanbakht, S.A. Alavi, H. Zilouei, Mechanisms of heavy metal removal using
444 microorganisms as biosorbent, *Water Sci. Technol.* 69 (2014) 1775–1787.
445 <https://doi.org/10.2166/wst.2013.718>.
- 446 [15] Q. Wang, Y. Wang, J. Tang, Z. Yang, L. Zhang, X. Huang, New insights into the interactions
447 between Pb(II) and fruit waste biosorbent, *Chemosphere.* 303 (2022) 135048.
448 <https://doi.org/10.1016/j.chemosphere.2022.135048>.
- 449 [16] B. Kayranli, O. Gok, T. Yilmaz, G. Gok, H. Celebi, I.Y. Seckin, O.C. Mesutoglu, Low-cost
450 organic adsorbent usage for removing Ni²⁺ and Pb²⁺ from aqueous solution and
451 adsorption mechanisms, *Int. J. Environ. Sci. Technol.* 19 (2022) 3547–3564.
452 <https://doi.org/10.1007/s13762-021-03653-z>.

- 453 [17] V. thi Quyen, T.H. Pham, J. Kim, D.M. Thanh, P.Q. Thang, Q. Van Le, S.H. Jung, T.Y. Kim,
454 Biosorbent derived from coffee husk for efficient removal of toxic heavy metals from
455 wastewater, *Chemosphere*. 284 (2021) 131312.
456 <https://doi.org/10.1016/j.chemosphere.2021.131312>.
- 457 [18] Z. Sheikh, M. Amin, N. Khan, M.N. Khan, S.K. Sami, S.B. Khan, I. Hafeez, S.A. Khan, E.M.
458 Bakhsh, C.K. Cheng, Potential application of *Allium Cepa* seeds as a novel biosorbent for
459 efficient biosorption of heavy metals ions from aqueous solution, *Chemosphere*. 279
460 (2021) 130545. <https://doi.org/10.1016/j.chemosphere.2021.130545>.
- 461 [19] W.M. Ibrahim, Y. S Abdel Aziz, S.M. Hamdy, N.S. Gad, Comparative Study for Biosorption
462 of Heavy Metals from Synthetic Wastewater by Different Types of Marine Algae, *J.*
463 *Bioremediation Biodegrad.* 09 (2018) 1–7. <https://doi.org/10.4172/2155-6199.1000425>.
- 464 [20] E. Romera, F. González, A. Ballester, M.L. Blázquez, J.A. Muñoz, Comparative study of
465 biosorption of heavy metals using different types of algae, *Bioresour. Technol.* 98 (2007)
466 3344–3353. <https://doi.org/10.1016/j.biortech.2006.09.026>.
- 467 [21] M. Gahlout, H. prajapati, P. Chauhan, L. Savande, P. Yadav, Isolation, screening and
468 identification of cyanobacteria and its uses in bioremediation of industrial effluents and
469 chromium sorption, *Int. J. Adv. Res. Biol. Sci.* 4 (2017) 138–146.
470 <https://doi.org/10.22192/IJARBS.2017.04.04.019>.
- 471 [22] A.P.S. Yadav, V. Dwivedi, S. Kumar, A. Kushwaha, L. Goswami, B.S. Reddy, Cyanobacterial
472 extracellular polymeric substances for heavy metal removal: A mini review, *J. Compos.*
473 *Sci.* 5 (2021) 1. <https://doi.org/10.3390/jcs5010001>.
- 474 [23] S.L.R.K. Kanamarlapudi, V.K. Chintalpudi, S. Muddada, Application of Biosorption for
475 Removal of Heavy Metals from Wastewater, *Biosorption*. (2018).
476 <https://doi.org/10.5772/intechopen.77315>.
- 477 [24] J. Wang, C. Chen, Biosorbents for heavy metals removal and their future, *Biotechnol.*
478 *Adv.* 27 (2009) 195–226. <https://doi.org/10.1016/j.biotechadv.2008.11.002>.

- 479 [25] C. Pennesi, C. Totti, T. Romagnoli, B. Bianco, I. De Michelis, F. Beolchini, Marine
480 Macrophytes as Effective Lead Biosorbents, *Water Environ. Res.* 84 (2012) 9–16.
481 <https://doi.org/10.2175/106143011x12989211841296>.
- 482 [26] M. Piccini, S. Raikova, M.J. Allen, C.J. Chuck, A synergistic use of microalgae and
483 macroalgae for heavy metal bioremediation and bioenergy production through
484 hydrothermal liquefaction, *Sustain. Energy Fuels*. 3 (2018) 292–301.
485 <https://doi.org/10.1039/C8SE00408K>.
- 486 [27] D. Inthorn, N. Sidtitoon, S. Silapanuntakul, A. Incharoensakdi, Sorption of mercury ,
487 cadmium and lead by microalgae, *ScienceAsia*. 28 (2002) 253–261.
- 488 [28] M. Blanco-Vieites, D. Suárez-Montes, F. Delgado, M. Álvarez-Gil, A.H. Battez, E.
489 Rodríguez, Removal of heavy metals and hydrocarbons by microalgae from wastewater
490 in the steel industry, *Algal Res.* 64 (2022) 102700.
491 <https://doi.org/10.1016/j.algal.2022.102700>.
- 492 [29] L.C. Ajjabi, L. Chouba, Biosorption of Cu²⁺ and Zn²⁺ from aqueous solutions by dried
493 marine green macroalga *Chaetomorpha linum*, *J. Environ. Manage.* 90 (2009) 3485–3489.
494 <https://doi.org/10.1016/j.jenvman.2009.06.001>.
- 495 [30] M. Costa, B. Henriques, J. Pinto, E. Fabre, M. Dias, J. Soares, L. Carvalho, C. Vale, J.
496 Pinheiro-Torres, E. Pereira, Influence of toxic elements on the simultaneous uptake of
497 rare earth elements from contaminated waters by estuarine macroalgae, *Chemosphere*.
498 252 (2020) 126562. <https://doi.org/10.1016/j.chemosphere.2020.126562>.
- 499 [31] H. Znad, M.R. Awual, S. Martini, The Utilization of Algae and Seaweed Biomass for
500 Bioremediation of Heavy Metal-Contaminated Wastewater, *Molecules*. 27 (2022) 1275.
501 <https://doi.org/10.3390/molecules27041275>.
- 502 [32] D.L. Ramasamy, S. Porada, M. Sillanpää, Marine algae: A promising resource for the
503 selective recovery of scandium and rare earth elements from aqueous systems, *Chem.*
504 *Eng. J.* 371 (2019) 759–768. <https://doi.org/10.1016/j.cej.2019.04.106>.

- 505 [33] B. Bina, M. Kermani, H. Movahedian, Z. Khazaei, Biosorption and recovery of copper and
506 zinc from aqueous solutions by nonliving biomass of marine brown algae of *Sargassum*
507 *sp.*, *Pakistan J. Biol. Sci.* 9 (2006) 1525–1530.
508 <https://doi.org/10.3923/pjbs.2006.1525.1530>.
- 509 [34] P. Christmann, G. Lefebvre, Trends in global mineral and metal criticality: the need for
510 technological foresight, *Miner. Econ.* 1 (2022) 1–12. [https://doi.org/10.1007/s13563-](https://doi.org/10.1007/s13563-022-00323-5)
511 [022-00323-5](https://doi.org/10.1007/s13563-022-00323-5).
- 512 [35] W. Miyamoto, S. Kosai, S. Hashimoto, Evaluating metal criticality for low-carbon power
513 generation technologies in Japan, *Minerals.* 9 (2019) 95.
514 <https://doi.org/10.3390/min9020095>.
- 515 [36] T. Watari, K. Nansai, K. Nakajima, Review of critical metal dynamics to 2050 for 48
516 elements, *Resour. Conserv. Recycl.* 155 (2020) 104669.
517 <https://doi.org/10.1016/j.resconrec.2019.104669>.
- 518 [37] H.B.S. Womersley, *Handbook of phycological methods. Culture methods and growth*
519 *measurements*, Cambridge University Press, 1973. [https://doi.org/10.1016/0304-](https://doi.org/10.1016/0304-3770(81)90012-7)
520 [3770\(81\)90012-7](https://doi.org/10.1016/0304-3770(81)90012-7).
- 521 [38] A.K. Zeraatkar, H. Ahmadzadeh, A.F. Talebi, N.R. Moheimani, M.P. McHenry, Potential
522 use of algae for heavy metal bioremediation, a critical review, *J. Environ. Manage.* 181
523 (2016) 817–831. <https://doi.org/10.1016/j.jenvman.2016.06.059>.
- 524 [39] E. Fabre, B. Henriques, T. Viana, J. Pinto, M. Costa, N. Ferreira, D. Tavares, C. Vale, J.
525 Pinheiro-Torres, E. Pereira, Optimization of Nd(III) removal from water by *Ulva sp.* and
526 *Gracilaria sp.* through Response Surface Methodology, *J. Environ. Chem. Eng.* 9 (2021)
527 105946. <https://doi.org/10.1016/j.jece.2021.105946>.
- 528 [40] J.A.C. Radway, E.W. Wilde, M.J. Whitaker, J.C. Weissman, Screening of algal strains for
529 metal removal capabilities, *J. Appl. Phycol.* 13 (2001) 451–455.
530 <https://doi.org/10.1023/A:1011111711821>.

- 531 [41] T.A. Davis, B. Volesky, A. Mucci, A review of the biochemistry of heavy metal biosorption
532 by brown algae, *Water Res.* 37 (2003) 4311–4330. <https://doi.org/10.1016/S0043->
533 1354(03)00293-8.
- 534 [42] J.A. Dean, *Lange's Handbook Of Chemistry*, 15th ed., McGraw-Hill, Inc., 1999.
- 535 [43] P.X. Sheng, Y.P. Ting, J.P. Chen, L. Hong, Sorption of lead, copper, cadmium, zinc, and
536 nickel by marine algal biomass: Characterization of biosorptive capacity and investigation
537 of mechanisms, *J. Colloid Interface Sci.* 275 (2004) 131–141.
538 <https://doi.org/10.1016/j.jcis.2004.01.036>.
- 539 [44] T. Kiran Marella, A. Saxena, A. Tiwari, Diatom mediated heavy metal remediation: A
540 review, *Bioresour. Technol.* 305 (2020) 123068.
541 <https://doi.org/10.1016/j.biortech.2020.123068>.
- 542 [45] S.L. Corder, M. Reeves, Biosorption of nickel in complex aqueous waste streams by
543 cyanobacteria, *Appl. Biochem. Biotechnol.* 45–46 (1994) 847–859.
544 <https://doi.org/10.1007/BF02941854>.
- 545 [46] A. Çelekli, H. Bozkurt, Bio-sorption of cadmium and nickel ions using *Spirulina platensis*:
546 Kinetic and equilibrium studies, *Desalination.* 275 (2011) 141–147.
547 <https://doi.org/10.1016/j.desal.2011.02.043>.
- 548 [47] A.E. Martell, R.M. Smith, *Other Organic Ligands*, 1st ed., Springer New York, NY, 1977.
549 <https://doi.org/10.1007/978-1-4757-1568-2>.
- 550 [48] R.M. Smith, A.E. Martell, *Critical Stability Constants: Inorganic Complexes*, 1975.
551 <https://doi.org/10.1007/978-1-4613-4452-0>.
- 552 [49] A.E. Martell, R.M. Smith, *Critical stability constants: Amino acids*, Plenum Press, New
553 York; London, 1974.
- 554 [50] H. Irving, R.J.P. Williams, Order of Stability of Metal Complexes, *Nat.* 1948 1624123. 162
555 (1948) 746–747. <https://doi.org/10.1038/162746a0>.
- 556 [51] H. Irving, R.J.P. Williams, The stability of transition-metal complexes, *J. Chem. Soc.* (1953)

- 557 3192–3210. <https://doi.org/10.1039/JR9530003192>.
- 558 [52] H. Köppel, D.R. Yarkony, H. Barentzen, The Jahn - Teller Effect - Fundamentals and
559 Implications for Physics and Chemistry, Springer Ser. Chem. Phys. 97 (2010) 912.
560 <http://link.springer.com/10.1007/978-3-642-03432-9>.
- 561 [53] R. Peñalver, J.M. Lorenzo, G. Ros, R. Amarowicz, M. Pateiro, G. Nieto, Seaweeds as a
562 functional ingredient for a healthy diet, Mar. Drugs. 18 (2020).
563 <https://doi.org/10.3390/md18060301>.
- 564 [54] I. Michalak, M. Mironiuk, K. Marycz, A comprehensive analysis of biosorption of metal
565 ions by macroalgae using ICP-OES, SEM-EDX and FTIR techniques, PLoS One. 13 (2018).
566 <https://doi.org/10.1371/journal.pone.0205590>.
- 567